

Hematopoietic stem cell gene therapy ameliorates CNS involvement in murine model of GM1-gangliosidosis

Toshiki Tsunogai,^{1,2} Toya Ohashi,⁶ Yohta Shimada,² Takashi Higuchi,² Ayaka Kimura,³ Ayako M. Watabe,⁴ Fusao Kato,⁵ Hiroyuki Ida,¹ and Hiroshi Kobayashi^{1,2}

¹Department of Pediatrics, The Jikei University School of Medicine, Tokyo, Japan; ²Division of Gene Therapy, Research Center for Medical Sciences, The Jikei University School of Medicine, Tokyo, Japan; ³Dementia Research Unit, Osaka Psychiatric Research Center, Osaka Psychiatric Medical Center, Osaka, Japan; ⁴Institute of Clinical Medicine and Research, Research Center for Medical Sciences, The Jikei University School of Medicine, Tokyo, Japan; ⁵Division of Neuroscience, Research Center for Medical Sciences, The Jikei University School of Medicine, Tokyo, Japan; ⁶Department of Human Health Science and Therapeutics, The Jikei University School of Nursing, Tokyo, Japan

GM1-gangliosidosis is a progressive neurodegenerative glycosphingolipidosis resulting from a *GLB1* gene mutation causing a deficiency of the lysosomal enzyme β -galactosidase, which leads to the abnormal accumulation of GM1 ganglioside in the central nervous system. In the most severe early infantile phenotype, excessive ganglioside accumulation results in a rapid decline in neurological and psychomotor functions, and death occurs within 2 years of age. Currently, there is no effective therapy for GM1-gangliosidosis. In this study, we evaluated the therapeutic efficacy of *ex vivo* gene therapy targeting hematopoietic stem cells using a lentiviral vector to increase enzyme activity, reduce substrate accumulation, and improve astrogliosis and motor function. Transplanting *GLB1*-transduced hematopoietic stem cells in mice increased β -galactosidase enzyme activity in the central nervous system and visceral organs. Specifically, this gene therapy significantly decreased GM1 ganglioside levels in the brain, especially in the cerebrum. More important, this gene therapy rectified astrogliosis in the cerebrum and improved motor function deficits. Furthermore, the elevation of serum β -galactosidase activity in secondary-transplanted mice suggested the ability of transduced hematopoietic stem cells to repopulate long term. These data indicate that *ex vivo* gene therapy with lentiviral vectors is a promising approach for the treatment of brain deficits in GM1 gangliosidosis.

INTRODUCTION

GM1 gangliosidosis (MIM: 230500) is an autosomal recessive lysosomal storage disorder (LSD) caused by mutations in the *GLB1* gene encoding lysosomal acid β -galactosidase (β gal), which hydrolyzes the terminal β -galactosyl residues of GM1 ganglioside, glycoproteins, and glycosaminoglycans.¹ Deficiency of β gal results in the accumulation of GM1 ganglioside and its asialo derivative GA1 in the central nervous system (CNS).² In the visceral organs, it results in the accumulation of partially degraded keratan sulfate, oligosac-

charides, and glycoproteins,³ causing skeletal dysplasia, hepatosplenomegaly, and cardiomyopathy. There are three main clinical variants: early infantile (type I), late-infantile/juvenile (type II), and adult (type III), categorized by severity and onset of symptoms.⁴ The early infantile form, the most severe subtype, with a profound reduction of enzyme activity, is characterized by early-onset (3–6 months), with a rapid decline in neurological functions. As the disease progresses, the patient dies within 2 years of age.⁴ In other forms, clinical features are either milder or absent, depending on the residual enzyme activity level.⁴ Currently, no effective treatment for GM1 gangliosidosis is available.

Viral vectors are potent tools for the transduction of therapeutic genes into various cells, and several gene therapy approaches have been tested in GM1 gangliosidosis animal models using adenovirus,⁵ oncoretrovirus,⁶ and adeno-associated virus (AAV) vectors.^{7–10} β gal secreted from genetically modified cells are taken into various cells by “cross-correction” via a mannose-6-phosphate receptor on the cell surface to function as a functional lysosomal enzyme. This uptake mechanism is key to gene therapy approaches for LSD, enabling active lysosomal enzymes to be distributed throughout the body. For type II GM1 gangliosidosis, a Phase I/II clinical trial to study the safety and efficacy of a single-dose gene transfer vector AAV9/*GLB1* by intravenous infusion (ClinicalTrials.gov: NCT 03952637) is ongoing. However, AAV-mediated gene transfer has a few drawbacks, such as limited cloning capacity,¹¹ host immunity to the vector,¹² and unknown sustainability. Since LSDs cause damage to a broad region of the CNS, it is expected that the topical administration of AAV will not be able to treat the entire brain.

Received 30 November 2021; accepted 25 April 2022;
<https://doi.org/10.1016/j.omtm.2022.04.012>

Correspondence: Toya Ohashi, Department of Human Health Science and Therapeutics, The Jikei University School of Nursing, Tokyo, Japan.
E-mail: tohashi@jikei.ac.jp



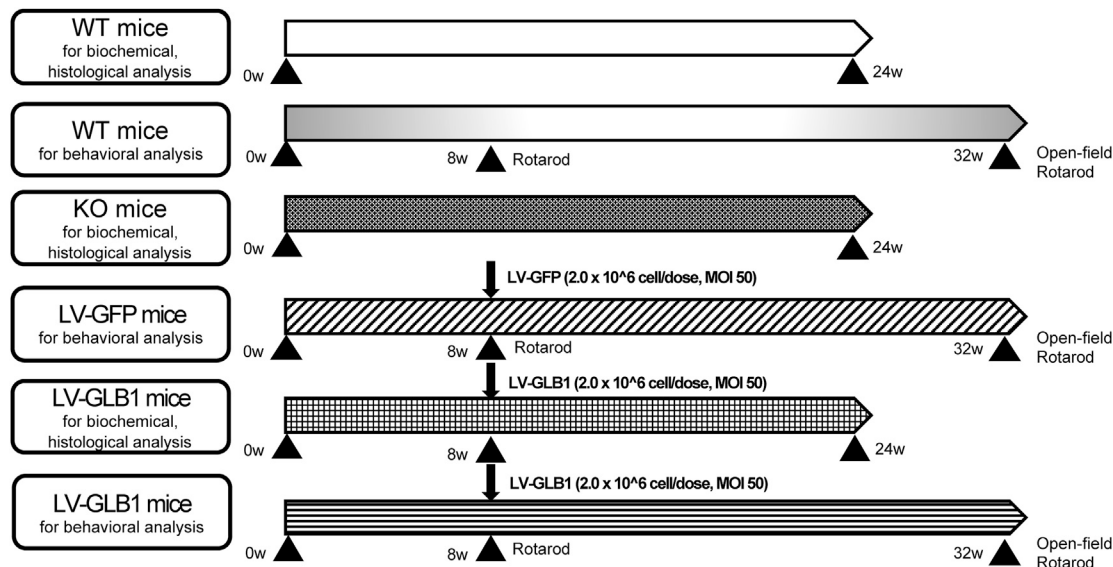


Figure 1. The scheme of procedure protocol

We formed 4 different groups, WT (wild-type) mice, KO ($\beta\text{gal}^{-/-}$) mice, LV-GFP (LV-SMPUR-MCU3-EGFP-treated $\beta\text{gal}^{-/-}$) mice, and LV-GLB1 (LV-SMPUR-MCU3-cGLB1-treated $\beta\text{gal}^{-/-}$) mice. For biological and histological analyses, we irradiated LV-GLB1 mice with 9 Gy at 8 weeks old, and at 24 weeks old, we harvested plasma, brain, liver, spleen, and bone marrow. For behavioral analysis, we irradiated LV-GLB1 and LV GFP mice with 9 Gy at 8 weeks old. Rotarod was performed at 8 weeks old (before the irradiation), and at 32 weeks old, an open field test was performed at 30 weeks old.

Lentiviral vector (LV)-mediated *ex vivo* hematopoietic stem cell gene therapy (HSC-GT) may be suitable for a systematic disease such as LSD compared to AAV gene therapy. It has been tested in an animal model of LSD, such as metachromatic leukodystrophy,¹³ mucopolysaccharidosis (MPS) type I,¹⁴ MPS type II,^{15–18} and MPS type IIIA.¹⁹ In humans, *ex vivo* gene therapy for metachromatic leukodystrophy provided evidence of the safety and therapeutic benefit of HSC-GT,²⁰ and has already been approved by the European Medicines Agency. It appears that enhanced secretion of βgal from HSCs is an attractive approach to ameliorate CNS lesions in GM1 gangliosidosis, but the effect has not yet been clarified. In this study, we assessed the therapeutic efficacy of HSC-targeted *ex vivo* gene therapy in GM1 gangliosidosis mice using LV-expressing mouse lysosomal βgal .

RESULTS

Overview of the study

We obtained lineage-negative cells from 8- to 12-week-old donor $\beta\text{gal}^{-/-}$ mice (2.0×10^6 cells/mouse), transduced at a multiplicity of infection of 50 with LV carrying the codon-optimized mouse GLB1 gene (cGLB1) or enhanced green fluorescent protein (EGFP) gene. For the recipient, mice were conditioned with 9 Gy lethal total body irradiation 24 h before the injection of the transduced cells. For biochemical and histological analysis, mice were terminated at 24 weeks of age ($n = 12$ for wild-type [WT] mice, $n = 10$ for $\beta\text{gal}^{-/-}$ [knockout, KO] mice, $n = 10$ for LV-SMPUR-MCU3-cGLB1-treated $\beta\text{gal}^{-/-}$ [LV-GLB1] mice). For the behavioral study, rotarod was conducted at 8 and 32 weeks, and the open-field test was conducted at 30 weeks ($n = 7$ for WT mice, $n = 6$ for LV-GLB1

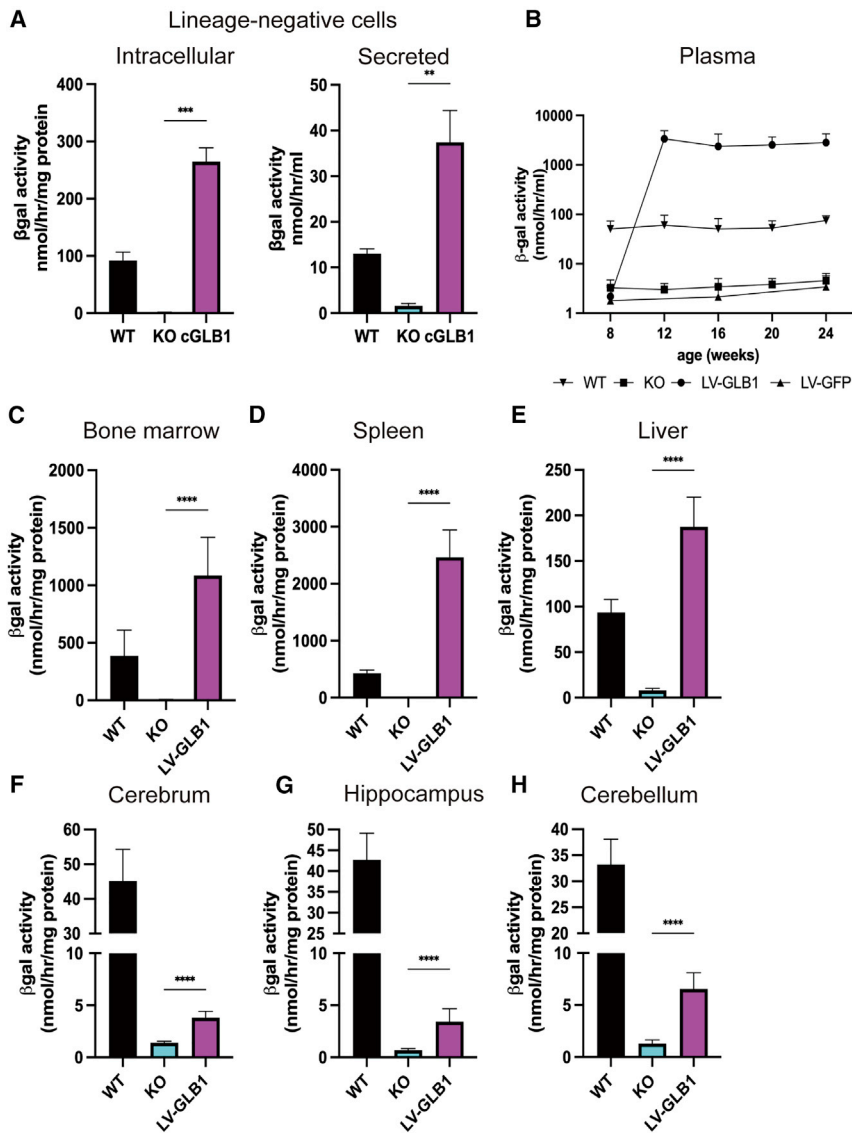
mice, and $n = 6$ for LV-SMPUR-MCU3-eGFP treated $\beta\text{gal}^{-/-}$ [LV-GFP] mice) (Figure 1).

The characteristic of the LV-transduced donor HSCs

To investigate the effect of lentiviral gene delivery to HSCs, we transduced lineage-negative cells derived from $\beta\text{gal}^{-/-}$ mouse bone marrow cells with a LV encoding cGLB1 and analyzed the activities of the enzyme. Cells were transduced at a multiplicity of infection (MOI) of 50 with LV-SMPUR-MCU3-cGLB1 (titer 9.0×10^9 IU/mL), and cells and media were collected 72 h later. Lentiviral gene transduction increased βgal enzyme activity in lineage-negative cells and media (Figure 2A).

Lentiviral *ex vivo* HSC gene therapy increases βgal activities in $\beta\text{gal}^{-/-}$ mouse

We evaluated βgal activity in the plasma and organs of LV-GLB1 ($n = 10$), LV-GFP ($n = 6$), KO ($n = 10$), and WT mice ($n = 12$) (Figures 2B–2H). From 4 weeks after transplantation, the level of βgal activity in plasma increased dramatically (50-fold higher than WT mice) in LV-GLB1 mice and remained elevated for 16 weeks after transplantation at 8 weeks old (Figure 2B). Since no increase in enzyme activity was observed between the LV-GFP group and the KO group, it can be assumed that the LV-GFP group will follow the same biochemical course as the KO group. In visceral organs (Figures 2C–2E, bone marrow cells, spleen, and liver), βgal activity was also increased in the LV-GLB1 mice (2- to 5-fold higher than WT mice). In the CNS tissue, βgal activity levels were significantly increased in the cerebrum ($p < 0.0001$), hippocampus ($p < 0.0001$), and cerebellum ($p < 0.0001$) than in KO mice. βgal activity levels were restored to 8.4%, 8.0%, and

**Figure 2. β gal activity systemic organs**

(A) Lineage-negative cells of KO mice were transduced at an MOI of 50 with LV-SMPUR-MCU3-cGLB1; after 72 h the enzyme activity was measured in cells and media. (B–H) β gal activities in various tissues were analyzed at 24 weeks old (16 weeks after transplantation). (B) Plasma, (C) bone marrow, (D) spleen, (E) liver, (F) cerebrum, (G) hippocampus, and (H) cerebellum. The β gal activities were expressed as nanomoles per hour per milliliter of plasma and as nanomoles per hour per milligram of protein in tissues. The results are shown as means \pm SEMs. The statistical analysis was performed by unpaired Student's t test. Two groups at the edge of the horizontal line indicate a significant difference, * $p < 0.05$, ** $p < 0.01$, *** $p < 0.001$, **** $p < 0.0001$.

side also tended to decrease in the hippocampus ($p = 0.08$). Next, to assess GM1 ganglioside storage in the brain histologically, we stained tissue sections (cerebral cortex [M1], hippocampus [CA1], and cerebellum) from LV-GLB1 mice, KO mice, and WT mice with cholera toxin B (CTX-B) (Figure 3D), and fluorescence intensity was quantitatively analyzed by ImageJ ($n = 3$; Figure 3E). In KO mice, almost every neuron was colocalized with CTX-B⁺ GM1 ganglioside, which was absent in WT mice in all three regions. In LV-GLB1 mice, for the cerebral cortex and cerebellum regions, the CTX-B⁺ areas were decreased compared to KO mice, indicating a reduction in ganglioside content, especially in the surrounding neuronal nuclei. In the hippocampus, the CTX-B⁺ area of the LV-GLB1 mice showed a marginal reduction compared to that in KO mice. Quantitative evaluation of the fluorescence intensity of CTX-B showed a significant decrease in the cerebrum of LV-GLB1 mice compared to KO mice. No statistically significant reduction was observed in the hippocampus and cerebellum. The combined results of LC-MS/MS and CTX-B staining indicated that lentiviral *ex vivo* HSC gene therapy reduced but did not completely normalize the accumulation of gangliosides in the CNS in this instance.

19.7% in WT mice of the same organ (Figures 2F–2H). These results indicated that *ex vivo* gene therapy increased β gal activity not only in peripheral tissues but also in the CNS of GM1 gangliosidosis mice.

Lentiviral *ex vivo* HSC gene therapy reduces the accumulation of GM1 ganglioside in the CNS

We analyzed the amounts and distribution of GM1 ganglioside in different brain regions of LV-GLB1 mice and compared them with those in age-matched WT and KO mice using liquid chromatography-tandem mass spectrometry (LC-MS/MS) and immunofluorescence staining. In the LC-MS/MS analysis (LV-GLB1 $n = 10$, KO $n = 10$, and WT $n = 12$), a significant reduction in GM1 ganglioside isoforms (C18) was observed in the cerebrum ($p = 0.0003$) and cerebellum ($p < 0.0001$) of LV-GLB1 mice compared to KO mice (Figures 3A–3C). Although not statistically significant, GM1 ganglio-

Ex vivo gene therapy and astrocytosis/myelination response in β gal^{-/-} mice

We evaluated the astrocytosis in the brain by identifying astrocytes using immunobiological labeling with an anti-gial fibrillary acidic protein (GFAP) antibody (Figure 4A), and the fluorescence intensity was quantitatively analyzed by ImageJ ($n = 3$; Figure 4B). In KO mice, there was an increase in GFAP⁺ areas in the cerebral cortex, cerebellum, and hippocampus, indicating that astrocytosis was induced. In the LV-GLB1 mice, there was a decrease in the GFAP⁺ area in the cerebral cortex and cerebellum, but no noticeable reduction was

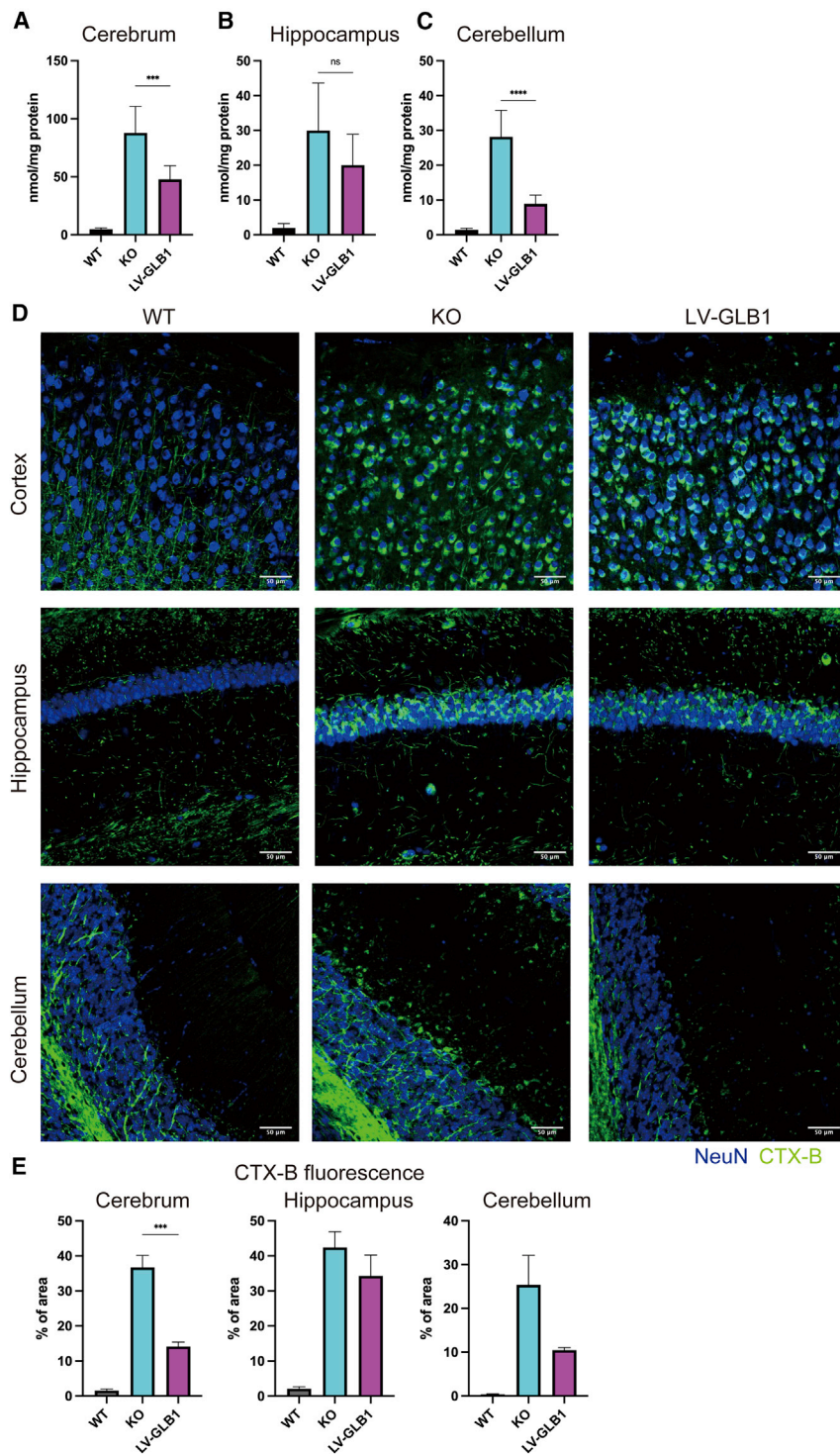


Figure 3. GM1 ganglioside content storage in the CNS
 GM1 ganglioside storage of the cerebrum, hippocampus, and cerebellum was evaluated by LC-MS/MS and immunostaining. (A–C) GM1 ganglioside content in the cerebrum (A), hippocampus (B), and cerebellum (C) of the WT, KO, and LV-GLB1 measured by LC-MS/MS. Results are shown as means ± SEMs. (D) Immunostaining of selected brain regions (cerebrum, hippocampus, and cerebellum). Stained with NeuN (blue) and CTX-B (green). Scale bar, 50 μm. (E) Immunostaining of selected brain regions (cerebrum, hippocampus, and cerebellum) with CTX-B was quantified by using ImageJ. The statistical analysis was performed by unpaired Student’s t test. Two groups at the edge of the horizontal line indicate a significant difference, *p < 0.05, **p < 0.01, ***p < 0.001, ****p < 0.0001.

expression levels of GFAP in the LV-GLB1, KO, and WT mice (n = 3) (Figures 4C and S1). The results showed an increase in GFAP in KO mice compared to WT mice in all three regions. In the LV-GLB1 group, a significant decrease was observed only in the cerebrum compared to that in KO mice. There were no statistically significant changes in the cerebellum and hippocampus compared to those in the KO mice.

Another feature of CNS damage in LSD is axonal injury/demyelination.^{4,21} The extent of demyelination was assessed using the anti-myelin basic protein (MBP) antibody (Figure S2). In the cerebral cortex, KO mice showed an apparent decrease in MBP⁺ myelin findings compared to WT mice. In LV-GLB1 mice, the MBP⁺ area was increased compared to that in KO mice.

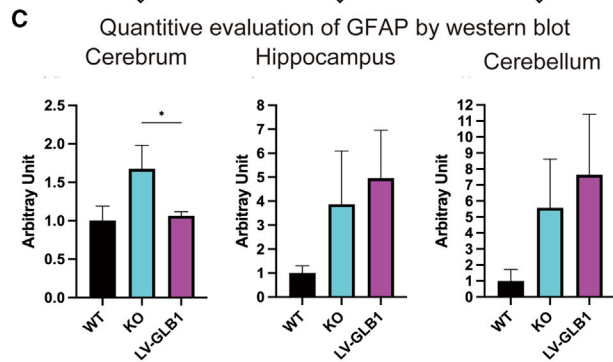
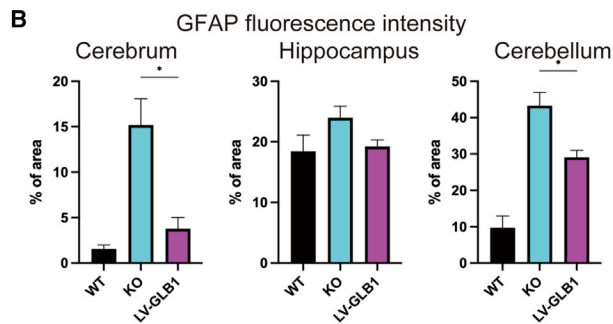
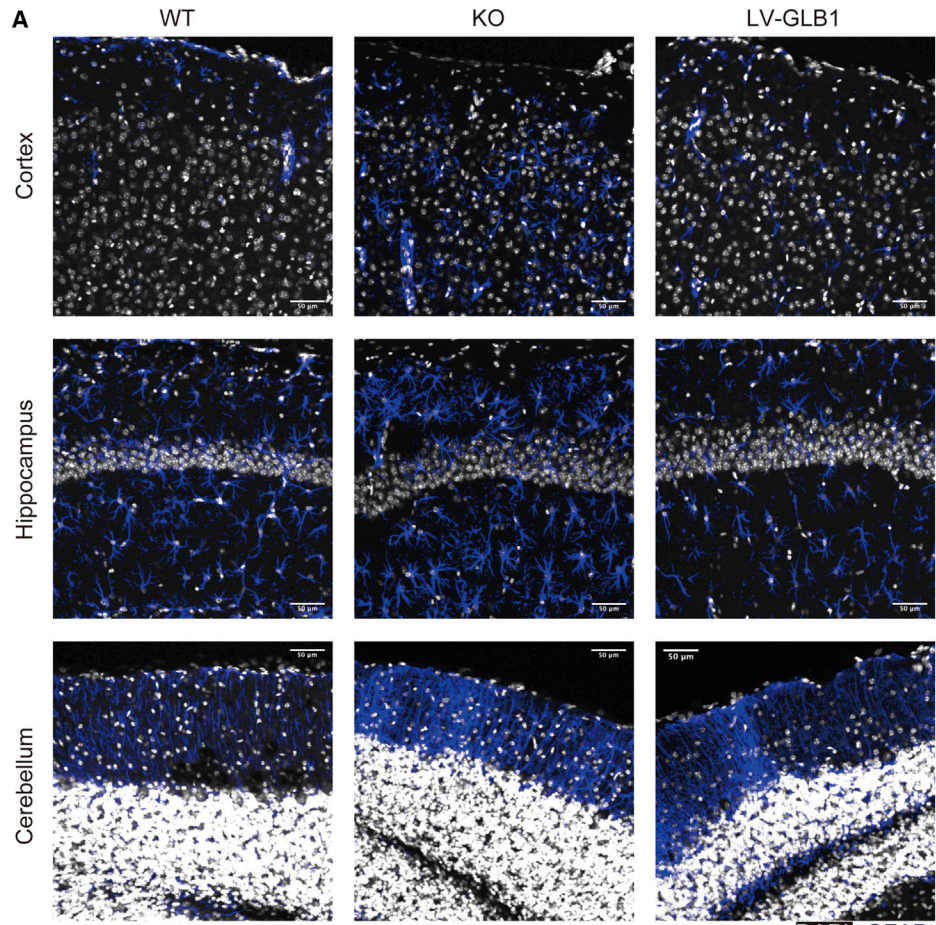
Ex vivo gene therapy effect on neurological function

To evaluate the neurological function in βgal^{-/-} mice and the efficiency of transplanted gene-modified HSCs, we conducted two types of behavioral tests: a rotarod test for motor coordination and an open-field test for locomotor activity and general anxiety, on LV-GLB1 mice (n = 6), LV-GFP mice (n = 6), and WT mice (n = 7).

There was no difference between KO and WT mice at 8 weeks of age in the rotarod test. At 16 and 24 weeks, LV-GFP and LV-GLB1 mice exhibited a decrease in motor function compared to WT mice. At 32 weeks, LV-GLB1 mice exhibited significantly longer latency to fall from the rotarod compared to LV-GFP mice (Figure 5A).

In the open-field test at 30 weeks, the total traveling distance and moving speed of LV-GLB1 and LV-GFP mice were lower than those of the WT mice, suggesting the

observed in the hippocampus (Figure 4A). The result of the quantitative analysis of fluorescence intensity was in line with the immunofluorescence image result (Figure 4B). To quantitatively evaluate the above results, western blotting was performed to determine the



(legend on next page)

deterioration of locomotor activity in both treated and KO mice, which cannot be ameliorated by gene therapy (Figures 5B and 5C). The percentages of time spent in the central region of the open-field arena and total movement duration were indistinguishable among all groups, suggesting that anxiety-related behavior was not affected among them (data not shown). The result of the rotarod test suggested that improvement in motor function was achieved after treatment, but was not completely normalized.

Biodistribution of the LV after *ex vivo* gene therapy

Real-time PCR ($n = 5$ for each) was performed in leukocytes, bone marrow cells, spleen, liver, cerebrum, and cerebellum to evaluate whether LV-transduced HSCs could engraft in transplanted mice and then be widely distributed in the central and peripheral organs (Figure 6A). The results showed that the virus was detected not only in peripheral organs but also in the CNS, indicating that it was widely distributed throughout the body.

Gene-corrected HSCs and their translocation into the brain

To determine whether the transplanted HSCs migrated to the CNS and differentiated into microglia-like cells, we performed immunostaining of the cerebral cortex of LV-GFP mice using a microglia/macrophage-specific anti-Iba1 antibody to analyze the localization of EGFP and microglia-like cells in the cerebral tissue (Figure 6B). EGFP fluorescence was observed in the cerebral cortex and was colocalized with Iba1⁺ cells, mainly in layers II/III. A similar result was observed in the hippocampus and cerebellum. These results strongly suggest that transplanted monocytes either migrate into the cerebrum or blood vessels surrounding the region and play a role in the therapeutic effect in CNS disease in GM1 mice.

Secondary transplantation

To evaluate the long-term repopulating ability of transduced HSCs, secondary transplantation using bone marrow cells from LV-GLB1 mice (32 weeks after transplantation) was conducted. We evaluated the enzyme activity in the plasma, liver, spleen, bone marrow, and cerebrum of these mice 16 weeks after transplantation ($n = 5$). Consequently, the enzyme activity in all five organs was increased, indicating that long-term repopulating cells were efficiently transduced by LV (Figure 7).

DISCUSSION

Here, we show that *ex vivo* HSC gene therapy with LV ameliorates biochemical and pathological abnormalities in the CNS of GM1 gangliosidosis with reduced deterioration of motor functions. To our knowledge, this is the first report to show that *ex vivo* gene therapy with LV can ameliorate CNS disease in GM1 gangliosidosis.

Our study showed that LV *ex vivo* HSC gene therapy increased the levels of β gal activity in the cerebrum and peripheral tissues of GM1 gangliosidosis mice. In HSC transplant (HSCT)-effective LSDs, such as metachromatic leukodystrophy (MLD) and mucopolysaccharidosis type I (MPS I), transplanted HSCs pass through the blood-brain barrier (BBB) and differentiate into microglial cells in the brain, thereby improving neuropathic disorders.²² Indeed, we found the presence of vector sequences in genomic DNA from the cerebral tissues of LV-GLB1 mice, and also detected the colocalization of GFP⁺ cells with microglia/macrophage marker Iba1⁺ cells in the cerebrum of LV-GFP mice. Therefore, as a known fact, we confirmed that the transplanted HSCs passed through the BBB and reached the cerebral tissues and then differentiated into Iba1⁺ microglia-like cells (or macrophages entered from the blood vessel to the brain parenchyma), which secrete enzymes, and the enzyme is incorporated into surrounding neurons and other cells by cross-correction in the GM1 gangliosidosis model mouse. Another factor could be that the enzyme overexpressed in the serum penetrated the BBB and reached the CNS, as it was previously reported that the administration of a high dose of enzyme resulted in a high level of the enzyme in serum, which penetrates BBB in MPS II and VII mice.^{23,24}

As a result of elevated enzyme activity in the CNS, there was a significant decrease in substrate accumulation in the brain, 40% in the cerebrum and hippocampus, and 70% in the cerebellum when compared to KO mice, but complete normalization was not achieved. It was reported that in several LSDs, such as MPS IIIA and GM1 gangliosidosis, at least 10% of normal enzyme activity is required to clear the substrate accumulation and prevent disease onset in an *in vitro* study.^{25,26} For MPS IIIA, achieving 10% of normal enzyme activity after *ex vivo* gene therapy was sufficient to normalize substrate accumulation, and a significant improvement in behavioral correction was obtained.¹⁹ For GM1 gangliosidosis, our *ex vivo* gene therapy achieved nearly 10% in the cerebrum but could not completely wash out the substrate storage. Sano et al. also reported *ex vivo* gene therapy with onco-retrovirus in a GM1 gangliosidosis mouse model, and the results showed increased β gal activity in different brain lesions and reduced GM1-ganglioside to some extent,⁶ which was very similar to our result. This difference between the degree of increase in enzyme activity and therapeutic effect for substrate reduction may be caused by the difference in the amount of enzyme required for normalization, which varies from cell to cell or from disease to disease. In our study, another possible reason for incomplete substrate reduction may be due to the timing of the transplant. GM1 gangliosidosis model mice begin to show progressive motor dysfunction and weight loss at approximately 16 weeks of age.²⁷ We expected that *ex vivo* gene therapy at 8 weeks of age, before the onset of

Figure 4. Neuropathologic features

Astrogliosis was evaluated with immunostaining and western blot using anti-GFAP antibody. (A) GFAP (blue) and DAPI (white) staining in the cerebrum, hippocampus, and cerebellum. Scale bar, 50 μ m. (B) Immunostaining of selected brain regions (cerebrum, hippocampus, and cerebellum) with GFAP was quantified by using ImageJ. (C) Quantitative analysis of western blot (cerebrum, hippocampus, and cerebellum). The values are shown as means \pm SEMs. The statistical analysis was performed by unpaired Student's *t* test. Two groups at the edge of the horizontal line indicate a significant difference, * $p < 0.05$, ** $p < 0.01$, *** $p < 0.001$, **** $p < 0.0001$.

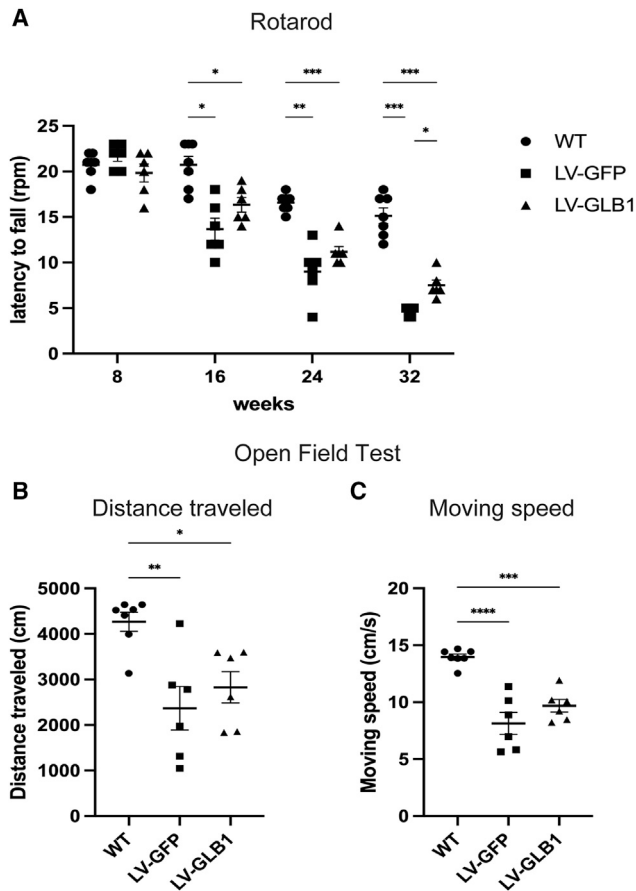


Figure 5. Behavioral performance

Behavioral evaluation with rotarod test and open field test was conducted. (A) Rotarod testing: Highest latency achieved on 4–40 rpm accelerating rotarod over 300 s over 3 trials. (B–C) Open field test. Total distance traveled (B) and moving speed (C) were analyzed. The results are shown as means \pm SDs. Two groups at the edge of the horizontal line indicate a significant difference, * $p < 0.05$, ** $p < 0.01$, *** $p < 0.001$, **** $p < 0.0001$ (1-way ANOVA, followed by Tukey-Kramer post hoc test).

symptoms, would suppress disease progression and promote rescue from dysfunction. However, the pathology of this model mouse shows granules in the neurons in the first few days of life, and vacuoles in the cell membrane begin to appear at 1–2 weeks, and by 8 weeks of age, there are, to some degree, pathological changes in all areas of the CNS.²⁸ From this, we speculate that by the time of treatment, a certain amount of substrate was already accumulated enough to cause invisible pathological change. Thus, *ex vivo* gene therapy at 8 weeks will not reverse the pathological damage that already exists; earlier intervention, before the occurrence of pathological change, should be important.

In this study, we found that the cerebellum profoundly increased enzyme activity and decreased GM1 ganglioside compared to the cerebellum and hippocampus. This phenomenon was also observed in *ex vivo* onco-retrovirus- or lentivirus-mediated gene therapy for

GM1 gangliosidosis⁶ and other LSD model mice, such as MPS II¹⁷ and MLD;^{13,29} however, the reason for this remains unclear. Previous reports have shown that the cerebellum and thalamus in GM1 gangliosidosis mouse models express more pro-inflammatory cytokines and chemokines than other CNS regions,⁶ suggesting that local inflammatory changes, cytokines, and chemokines trigger the recruitment of monocytes. In the present study, we speculate that owing to the difference in the inflammatory environment, larger numbers of microglia-like cells may have been recruited into the cerebellum than to the cerebral cortex or hippocampus, resulting in increased enzyme activity and decreased substrate accumulation. In the MLD mouse model and *ex vivo* gene therapy, cells migrated from transplanted HSCs were evident in the cerebellum at an earlier stage than in the cerebrum. In other words, this may not be unique to GM1 gangliosidosis alone but may be true for *ex vivo* gene therapy for LSDs in general. This phenomenon is thought to be related to the structure of the BBB, differences in the cellular composition and neurotransmitter network of each brain region, or differences in whether the brain is located supratentorial, but the detailed mechanisms remain unclear. However, it is widely known that individual LSDs respond differently to the same therapy, mainly due to the different characteristics of the enzyme itself, accumulated substrate, or both. Therefore, for LSDs, it will be necessary to evaluate each therapy in animal models of each disease.

Our *ex vivo* gene therapy reduced the GM1 gangliosides storage, which may be effective to CNS disorders in GM1 gangliosidosis model mice but was not completely normalized. As mentioned above, the timing of intervention is key to the success; however, other factors could advance our therapy. One of these factors is the transduction rate. Although HSCs can produce an excess of enzymes from each cell differentiated from donor HSCs, if the transduction rate is not high, the effect may be limited. Using agents such as prostaglandin E2 or cyclosporine A/cyclosporine H has been reported to enhance the gene transfer efficiency of LV to HSCs.^{30–32} In addition, modifying secreted enzymes themselves, for example, instead of producing a normal enzyme, creates a novel enzyme that is fused with a signal that will penetrate the BBB to migrate into the brain.³³

GM1 gangliosidosis is a systemic disease including CNS. Systemic administration of AAV vector, even if it is neurodirectional, effect to CNS is very limited in human trial. Thus, to treat the CNS of LSDs using AAV, brain-directed administration is preferable. However, in this case, the effect on peripheral organs may be limited. Alternatively, HSC target gene therapy using LV can treat peripheral organs as well as the CNS. Moreover, AAV cannot be administered to seropositive patients. HSC target gene therapy using LV can be performed to seropositive patients. Chemical chaperones are small molecules that bind and stabilize misfolded proteins, which contribute to increasing the residual activity and are amenable to LSDs, such as Gaucher disease and Fabry disease.^{34,35} In GM1 gangliosidosis, oral administration of *N*-octyl-4-epi- β -valienamine (NOEV) in a model mouse expressing a mutant β gal enzyme protein R201C significantly enhanced enzyme activity in the brain and other tissues.³⁶ However,

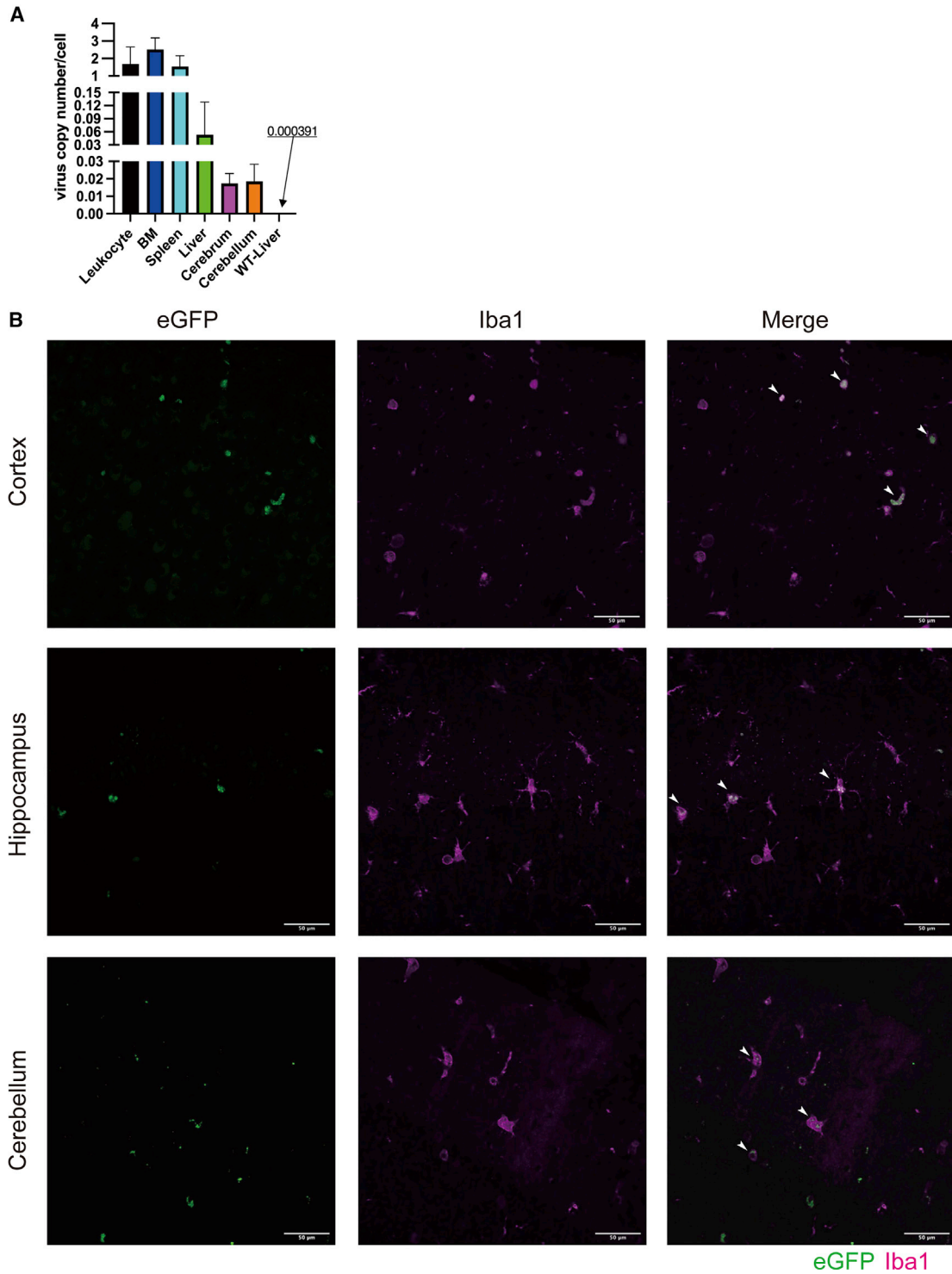


Figure 6. Biodistribution and engraftment of LV-GLB1 or LV-GFP transduced HSCs

(A) The biodistribution of the vector in organs (leukocyte, bone marrow, spleen, liver, cerebrum, cerebellum, and WT liver as control) was determined by quantitative PCR at 16 weeks after transplantation in LV SMPUR-MCU3-cGLB1. (B) The cerebral cortex, hippocampus, and cerebellum from LV-GFP mice were stained with an Iba1 (red).

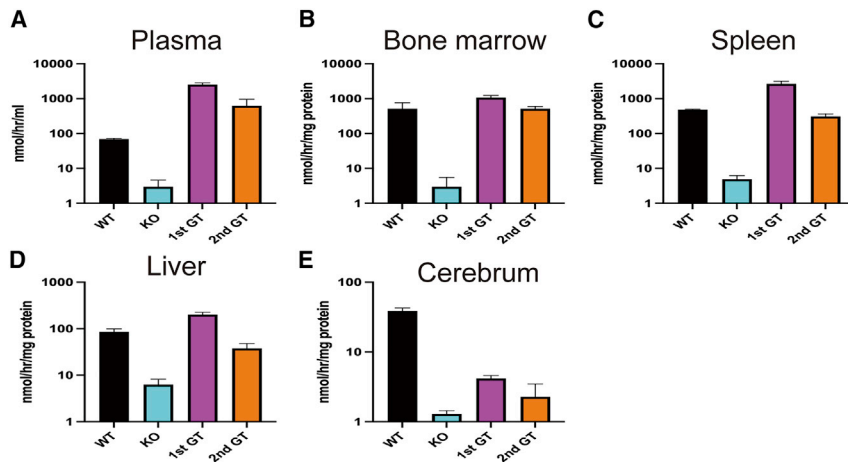


Figure 7. Secondary transplant

(A–E) Analysis of β gal activity in systemic tissues (plasma [A], bone marrow [B], spleen [C], liver [D], cerebrum [E]) of primary and secondary transplanted mice (1st GT and 2nd GT), compared with WT and KO mice ($n = 5$). The results are expressed as means \pm SEMs.

chemical chaperones work only in patients with amenable mutations. Our *ex vivo* gene therapy was indicated for all patients regardless of the mutations.

The limitations of this study include the lack of evaluation of safety issues associated with genotoxicity. Genotoxicity is an inextricable issue, especially with *ex vivo* gene therapy using an oncoretroviral vector. Leukemia develops because of the random integration of vector sequences in the host genome in gene therapy for X-linked severe combined immunodeficiency (X-SCID) and X-linked chronic granulomatous disease (XCGD).^{37,38} In addition, in β -thalassemia treated with LV *ex vivo* gene therapy, clonal expansion was observed.³⁹ Recently, reports of the long-term efficacy of LV-mediated GT in XCGD mouse models have demonstrated that the clinical background of the original disease may play an important role in carcinogenicity rather than random integration.⁴⁰ In addition, recent reports of leukemia after gene therapy for sickle cell disease have proposed that it was not due to the conditioning regimen busulfan or the insertional mutagenesis, but was caused by preexisting premalignant clones that were expanded by the stress of gene therapy. This genotoxicity is a very important issue, and we will conduct further evaluation and analysis of the integration sites and any preexisting premalignant characteristics in our future studies. In addition, in primary immunodeficiency such as X-linked SCID, gene-corrected cells gain a growth advantage over not-corrected cells. This may be one reason for the development of leukemia; however, growth advantage cannot be expected in lysosomal storage disease.

Also, staining with CTX-B may overestimate GM1 expression because of high affinity and broad cross-reactivity.⁴¹ Yanagisawa et al. noted that determining GM1 expression solely on cell staining with CTX-B could lead to an erroneous conclusion.⁴¹ Regarding this uncertainty, we analyzed GM1 accumulation not only with the fluorescence of CTX-B but also with GM1-ganglioside (C18) using LC-MS/MS. LC-MS/MS showed a significant C18 decrease in the cerebrum and cerebellum, but not in the hippocampus. Quantitative analysis of fluorescence of CTX-B in the cerebrum was significantly

decreased and not decreased in the hippocampus, which was in line with the results of the LC-MS/MS. For the cerebellum, CTX-B intensity seems to be reduced in the image, but not statically significant when quantified. This difference may be caused by the high affinity and broad cross-reactivity of CTX-B; however, the results of the LC-MS/MS and immunofluorescence showed similarity. Therefore, for this study, using

CTX-B staining together with biochemical analysis with LC-MS/MS was appropriate to evaluate substrate accumulation.

This is the first report of LV *ex vivo* gene therapy in a mouse model of GM1. We successfully increased enzyme activity broadly in the CNS and other peripheral organs, resulting in reduced GM1 ganglioside accumulation and improved neurological findings. To further improve the therapeutic effect, we need to investigate efficient transduction protocols for HSCs, an efficient delivery system of the enzyme to the CNS, and an efficient method to recruit microglia-like cells to the cerebra so that substrate levels can be normalized.

MATERIALS AND METHODS

Animals

β gal KO mouse (β gal^{-/-}), which was made by disrupting the mouse β gal gene in exon 15 by homologous recombination in embryonic stem cells²⁷ and heterogeneous mouse (β gal^{+/-}), were obtained originally from the Laboratory Animal Resource Bank at the National Institutes of Biomedical Innovation, Health, and Nutrition (NIBIOHN, Osaka, Japan). Mice for these experiments were generated by breeding β gal^{+/-} females with β gal^{+/-} males. Genotypes were determined by PCR.²⁷ The Institutional Animal Care and Use Committee of Jikei University approved all of the procedures, including animal experiments and husbandry.

For studies of GM1 gangliosidosis using a murine model, most were performed in β gal KO mice generated by Hahn et al.;⁴² however, we performed ours with β gal KO mice generated by Matsuda et al.²⁷ The β gal gene consists of 16 exons. Hahn et al. inactivated the β gal gene by inserting a neomycin-resistance gene into the middle of exon 6. Matsuda et al. inserted it into exon 15. Two model mice share very similar biochemical and pathological characteristics.

LV construction and production

The self-inactivating lentiviral plasmid vector pSMPUR-MCU3-MCS was provided by Dr. Donald B. Kohn (University of California, Los Angeles).⁴³ The vector has an MCU3 promoter, the U3 region from the MND promoter, a synthetic promoter containing the U3 region of a

modified Moloney murine leukemia virus long terminal repeat with a myeloproliferative sarcoma virus enhancer with substitution of the TATA site for that of the human CMV promoter.⁴⁴ The cGLB1 gene (GenScript, Piscataway, NJ) and EGFP gene were inserted into multiple cloning sites of the vector pSMPUR-MCU3-MCS to create pSMPUR-MCU3-cGLB1 or pSMPUR-MCU3-EGFP. Large-scale production of LVs was prepared following a previously described procedure.⁴³ Lentiviral titers were determined by enzyme-linked immunosorbent assay of the viral p24 protein.⁴⁵ The recombinant Gene Research Safety Committee of The Jikei University and the Jikei University Committee for Laboratory Biosafety approved all of the vector constructions and procedures for generating the lentivirus vector.

Transduction and transplantation of lineage-negative bone marrow cells

Whole bone marrow cells were harvested from the tibias and femurs of donor $\beta\text{gal}^{-/-}$ mice (8–12 weeks old) and concentrated HSCs using a lineage cell depletion kit (Miltenyi Biotec, Auburn, CA). Lineage-negative cells were transduced at a MOI of 50, with LV carrying cGLB1 (LV-GLB1) or EGFP (LV-GFP) genes for 24 h on a RetroNectin-coated 6-well plate (Takara Bio, Shiga, Japan) at a density of 2×10^6 cells/mL in Dulbecco's modified Eagle's medium (DMEM; Fujifilm, Wako Pure Chemical, Tokyo, Japan) with 10% fetal bovine serum (FBS; Thermo Fisher Scientific, Waltham, MA), recombinant mouse Flt-3 ligand (rnFlt3, 100 ng/mL; R&D Systems, Minneapolis, MN), and recombinant mouse stem cell factor (rmSCF, 100 ng/mL; R&D Systems).

To characterize transduced cells, the cells were washed with phosphate-buffered saline (PBS; Fujifilm Wako Pure Chemical) after 24 h of infection and continuously cultivated by 48 h after infection. βgal activity was assayed in cells and medium.

For the mice study, the infected cells were washed with PBS after 24 h and 2.0×10^6 cells were injected intravenously into $\beta\text{gal}^{-/-}$ recipient mice (8 weeks old) after lethal total body irradiation of 9 Gy using a Hitachi-MBR1520-R irradiator (Hitachi, Tokyo, Japan), according to a procedure previously described.⁴⁶

For secondary bone marrow transplant, whole bone marrow cells were harvested from the tibias and femurs of first transplanted $\beta\text{gal}^{-/-}$ recipient mice (36 weeks old) and injected intravenously into $\beta\text{gal}^{-/-}$ recipient mice (8 weeks old) after lethal irradiation of 9 Gy, as described earlier.

Sample collection and preparation

For the characterization of transduced cells, cultivated cells were homogenized with distilled water and centrifuged at 14,000 rpm for 10 min at 4°C, and the supernatants were stored at -80°C until the βgal assay. For the cultivated medium, it was collected and centrifuged at 14,000 rpm for 10 min at 4°C, and the supernatants were stored at -80°C until the βgal assay.

For the mice study, a blood sample was collected before conditioning and then every 4 weeks until 24 weeks of age by puncturing the super-

ficial temporal vein of the mice using a heparinized microcapillary tube. The collected blood was placed inside a microtube and centrifuged at 14,000 rpm for 10 min at 4°C, and the supernatants were stored as plasma samples at -80°C until all of the samples had been collected. At the termination of the study (16 weeks after transplantation), the mice were anesthetized by isoflurane inhalation (Pfizer, New York, NY) and perfused with 30 mL PBS. The brain, liver, spleen, and bone marrow were collected. The right hemisphere of the brain was separated into the cerebrum, hippocampus, and cerebellum for biochemical assays. The left hemisphere of the brain was dissected for histological analysis. The left hemisphere was fixed overnight in 4% paraformaldehyde (Fujifilm Wako Pure Chemical) at 4°C. For cryoprotection, the brain was placed in 30% sucrose in PBS overnight at 4°C, and then the brain was embedded in Tissue-Tek Optimal Cutting Temperature Compound (Sakura Finetek Japan, Tokyo, Japan) and stored at -80°C .

βgal activity analysis

Cells, medium, frozen tissues, and plasma samples were used for βgal analysis. Frozen tissues were homogenized in 6 volumes of distilled water and centrifuged at 14,000 rpm for 15 min at 4°C. The supernatant of cells, medium, frozen tissues, and plasma was used for the βgal assay. The total $\beta\text{-gal}$ activity was determined using 4-methylumbelliferyl- $\beta\text{-D-galactopyranoside}$ as the synthetic fluorogenic substrate, as previously described. Briefly, 100 μL of the medium, 10 μL plasma or 10 μg protein in tissue lysates were mixed with 4-methylumbelliferyl- $\beta\text{-D-galactopyranoside}$, and the mixture was incubated at 37°C for 1 h. The reaction was terminated by adding 3.98 mL stop buffer.⁴⁷ The total βgal assay was performed by measuring the release of 4-methylumbelliferone at 365 nm excitation and 460 nm emission on an RF 5300PC spectrofluorophotometer (Shimadzu, Kyoto, Japan). Protein concentrations were determined using the Pierce BCA Protein Assay Kit (Thermo Fisher Scientific) following the manufacturer's instructions. Enzymatic activity was expressed as either nanomoles per hour per milliliter (plasma and medium) or nanomoles per hour per milligram (tissues, normalized to total protein concentration).

Analysis of lentivirus copy number

DNA was extracted from leukocytes, cerebrum, cerebellum, liver, spleen, and bone marrow using a Maxwell 16 DNA Purification Kit (Promega, Madison, WI). The virus copy number was quantified by quantitative real-time PCR, as described, with minor modifications.⁴³ Briefly, 100 ng genomic DNA (1.67×10^4 genomes) was mixed with a TaqMan Universal PCR master mix containing 900 nM each of forward and reverse primers, and 250 nM lentiviral packaging sequence probe. TaqMan primers and probes were obtained from Thermo Fisher Scientific. The primers and probe sequences were as follows: forward primer, 5'-ACCTGAAAGCAGAAAGGGAAAC-3'; reverse primer, 5'-CACCCATCTCTCCTTCTAAGCC-3'; probe, 5'-FAM-AGCTCTCTCGACGCAGGACTCGGC-TAMRA-3'. The $\beta\text{-actin}$ internal control primers and probe sequences were as follows: forward primer, 5'-GGTCGTACCACAGGCATTGT-3'; reverse primer, 5'-CTCGTA GATGGCCACAGTGT-3'; probe, 5'-FAM-CCCGTCTCCGGAGTCC-TAMRA-3'. Ultrapure distilled water

was used as a negative control. Amplifications were performed in a QuantStudio 5 (Thermo Fisher Scientific), with initial denaturation for 10 min at 95°C, followed by 40 cycles of 15 s at 95°C and 60 s at 60°C. To calculate the copy number, a standard curve was generated using the linearized pSMPUR-MCU3-cGLB1 plasmid as a template. The copy number of the vector DNA was determined by comparing the threshold cycle (Ct) values of the samples to the plasmid standard reference curve.

Analysis of GM1 gangliosides content

High-performance liquid chromatography-MS/MS (HPLC-MS/MS) was used for the quantification of GM1-ganglioside in the CNS. Total lipids were extracted using the Folch method.⁴⁸ Briefly, tissues were homogenized with distilled water, followed by extraction with chloroform:methanol (2:1, v/v). The extracted samples were analyzed using LC-MS/MS (LCMS-8040, Shimadzu). A Synergi MAX-RP (150 mm × 4.6 mm, Phenomenex, Torrance, CA) was used for separation. The flow rate was 0.4 mL/min. Mobile phase A was distilled water (Kanto Chemical, Tokyo, Japan) containing 2 mM ammonium acetate (Fujifilm Wako Pure Chemical) and 0.1% formic acid (Nacalai Tesque, Kyoto, Japan). Mobile phase B consisted of methanol (Fujifilm Wako Pure Chemical) containing 2 mM ammonium acetate and 0.1% formic acid. The mobile phase gradients were as follows: 0–2 min, 100% B; 2–30 min, 100% B; and 30.1–31 min, 0% B. GM1 ganglioside isoforms were quantified by multiple reaction monitoring (MRM) in negative ion mode. The transitions are as follows: C16 (d18:1/16:0); m/z 1,517.35 > 290.1, C18 (d18:1/18:0); m/z 1,545.85 > 290.1, C20 (d18:1/24:0); m/z 1,573.45 > 290.1. The concentrations of these isoforms were calculated using a calibration curve of GM1 ganglioside (860065, Avanti Polar Lipids, Birmingham, AL).

Histological analysis

Cryoprotected fixed-frozen brain samples were sliced into 40- μ m thickness using a cryostat (CM 1950, Leica Biosystems Nussloch GmbH, Wetzlar, Germany). For immunohistochemistry, the sections were washed with PBS and incubated in a blocking buffer for 30 min at room temperature. The composition of the blocking buffer was as follows: 3% FBS and 1% Triton X (Sigma-Aldrich, St. Louis, MO) in PBS. The sections were then incubated with a blocking buffer containing primary antibodies for 18 h at 4°C. After washing with PBS three times, the sections were incubated in blocking buffer containing secondary antibodies and DAPI (1:500, Fujifilm Wako Pure Chemical) for 2–3 h at room temperature. The following primary antibodies and chemicals were used: Alexa 488-conjugated CTX-B (1:300, Thermo Fisher Scientific), chicken anti-GFAP (1:500, Millipore, Billerica, MA), rabbit anti-Iba1 (1:500, Fujifilm Wako Shibayagi), mouse anti-NeuN (1:500, Millipore), and rat anti-MBP (1:500, Abcam, Cambridge, UK). The following secondary antibodies and dilutions were used (all from Biotium, Fremont, CA): Alexa Fluor 488 donkey anti-rat (1:500), anti-chicken (1:500), Alexa Fluor 555 donkey anti-rabbit (1:500), anti-mouse (1:500), Alexa Fluor 647 donkey anti-mouse (1:500), and goat anti-chicken (1:500).

After the sections were washed with PBS three times and mounted, they were imaged using an Olympus FV1200 confocal laser scanning

inverted microscope (Olympus, Tokyo, Japan), which was equipped with 405-, 488-, 561-, and 640-nm lasers. CTX-B and GFAP immunofluorescence was quantified using ImageJ software ($n = 3/\text{group}$).

Western blot analysis

Western blot analysis was performed according to a previously described procedure with minor modifications.⁴⁹ Cerebral tissues were homogenized in 9 volumes of 50 mM Tris-HCl, pH 7.5 (Tris buffer), and protease inhibitor cocktail (PIC; Roche Diagnostics, Indianapolis, IN), followed by sonication and centrifugation at 18,000 × g for 1 h at 4°C. Residual pellets were lysed with 7 volumes of Tris buffer containing 2% sodium dodecyl sulfate (SDS) and PIC, followed by sonication and centrifugation. Samples containing equal amounts of proteins were resolved by SDS-PAGE on 4%–20% TGX (Tris-glycine extended) gels and transferred onto nitrocellulose membranes using the Trans-Blot Turbo System (Bio-Rad, Hercules, CA). The membranes were stained with Ponceau S (Nacalai, Tokyo) for the analysis of total proteins. After a brief wash, the membranes were dipped in a blocking buffer (Tris buffer containing 150 mM NaCl, 0.1% gelatin, 0.1% casein, and 0.05% Tween 20) and incubated with each primary antibody. Membranes were then immunostained with peroxidase-labeled secondary antibody (Nichirei, Tokyo, Japan) and analyzed using a Chemi Doc XRS + System and Image Lab software (Bio-Rad). Quantitative analysis of the target band was performed by normalizing the total protein.

Behavioral experiments

Mice were group housed (5–6 mice/cage) under a 12-h light/dark cycle and provided with water and food *ad libitum*. Rotarod testing was conducted using a Rotarod apparatus (LE8205, Panlab Harvard Apparatus, Barcelona, Spain) as follows. Animals were placed on an accelerating rotarod from 4 to 40 rpm over 5 min, and the latency to fall was recorded. Testing was conducted with 1 practice trial of 1 min at 2 rpm (or 30 s at 4 rpm 2 times if complex) before the session, followed by 3 trials with 15–20 min of rest in between for 3 consecutive days (total of 9 trials). The latency to fall for each mouse in a testing session was recorded, and the longest time on the rotarod in any of the nine trials was reported.

Open-field experiments were conducted on a square apparatus with gray walls (100×, 50 cm width × 50 cm depth × 30 cm height) (O'Hara, Tokyo, Japan). Each mouse was placed in the corner of the apparatus and allowed to freely explore the environment for a 10-min test session. During this time, the ambulation of the mice was recorded and analyzed using a video-computerized tracking system (TimeOFCR1, O'Hara). The total traveling distance (cm), time spent in the center region (%), total movement duration (s), and moving speed (cm/s) were recorded and analyzed as a proxy for basic locomotor activities and general anxiety levels, respectively. The entire open-field area was divided into 25 (5 × 5) square areas, and the central parts of any one of the 9 (3 × 3) areas over the surrounding peripheral 16 areas were expressed as the central region.

Statistical analysis

All of the data, except behavioral experiments, are reported as means ± standard deviations, and the data from the behavioral

experiments are reported as means \pm standard errors of the mean. All of the statistical analyses were performed using Prism 9 for MacOS (GraphPad Software, San Diego, CA, and Apple, Cupertino, CA). For data from β gal activity analysis, GM1 ganglioside content analysis, and western blot analysis, we used an unpaired t test to calculate the statistical significance between LV-GLB1 mice and KO mice. For behavioral experiments, one-way ANOVA with Tukey's test as a post hoc test was used to calculate statistical significance between LV-GFP, LV-GLB1 mice, and WT mice. The null hypothesis was that there was no difference in GM1 accumulation between the treated and untreated groups. Similarly, the null hypothesis about enzyme activity was that there was no difference in enzyme activity between the treated and untreated groups. Therefore, a comparison between the two groups was performed. Compared with WT mice, β gal activity is low in GM1 model mice, and it is widely known that GM1 is accumulated, so it is not included in this comparison. In the behavioral test, the GM1 model mouse had never been compared with the WT mouse, so the comparison was made between the three groups. Statistical significance was set at $p < 0.05$.

SUPPLEMENTAL INFORMATION

Supplemental information can be found online at <https://doi.org/10.1016/j.omtm.2022.04.012>.

ACKNOWLEDGMENTS

This work was supported by JSPS KAKENHI (grant no. JP18H02783). The authors are indebted to Dr. Donald B. Kohn (UCLA) for providing the LV. The authors thank Ms. Sayoko Iizuka, Ms. Natsumi Motoki, Ms. Aimi Yuasa, Ms. Yukari Takahashi, and Mr. Suguru Tohyama (the Jikei University School of Medicine) for their excellent technical assistance, and members of the Laboratory Animal Facility (The Jikei University School of Medicine) for their assistance with animal studies. We would like to thank Editage (www.editage.com) for English language editing.

AUTHOR CONTRIBUTIONS

T.T. and T.O. designed and conducted the research; T.T., Y.S., T.H., and A.K. performed the research and discussed the data. A.M.W. designed the behavioral experiments. F.K., H.I., and H.K. analyzed the results and edited the manuscript. T.T. wrote the manuscript.

DECLARATION OF INTERESTS

The authors declare no competing interests.

REFERENCES

- Okada, S., and O'Brien, J.S. (1968). Generalized gangliosidosis, beta-galactosidase deficiency. *Science* *160*, 1002–1004. <https://doi.org/10.1126/science.160.3831.1002>.
- O'Brien, J.S., Stern, M.B., Landing, B.H., O'Brien, J.K., and Donnell, G.N. (1965). Generalized gangliosidosis, another inborn error of ganglioside metabolism? *Am. J. Dis. Child.* *109*, 338–346. <https://doi.org/10.1001/archpedi.1965.02900020340014>.
- Suzuki, K. (1968). Cerebral GM1-gangliosidosis, chemical pathology of visceral organs. *Science* *159*, 1471–1472. <https://doi.org/10.1126/science.159.3822.1471>.
- Suzuki, Y., Oshima, A., and Nanba, E. (2008). β -Galactosidase deficiency (β -Galactosidosis): GM1 gangliosidosis and morquio B disease. *The Online Metabolic and Molecular Bases of Inherited Disease* (McGraw Hill), pp. 1–101.
- Takaura, N., Yagi, T., Maeda, M., Nanba, E., Oshima, A., Suzuki, Y., Yamano, T., and Tanaka, A. (2003). Attenuation of ganglioside GM1 accumulation in the brain of GM1 gangliosidosis mice by neonatal intravenous gene transfer. *Gene Ther.* *10*, 1487–1493. <https://doi.org/10.1038/sj.gt.3302033>.
- Sano, R., Tessitore, A., Ingrassia, A., and d'Azzo, A. (2005). Chemokine-induced recruitment of genetically modified bone marrow cells into the CNS of GM1-gangliosidosis mice corrects neuronal pathology. *Blood* *106*, 2259–2268. <https://doi.org/10.1182/blood-2005-03-1189>.
- Hinderer, C., Nosratbakhsh, B., Katz, N., and Wilson, J.M. (2020). A single injection of an optimized adeno-associated viral vector into cerebrospinal fluid corrects neurological disease in a murine model of GM1 gangliosidosis. *Hum. Gene Ther.* *31*, 1169–1177. <https://doi.org/10.1089/hum.2018.206>.
- Weismann, C.M., Ferreira, J., Keeler, A.M., Su, Q., Qui, L., Shaffer, S.A., Xu, Z., Gao, G., and Sena-Esteves, M. (2015). Systemic AAV9 gene transfer in adult GM1 gangliosidosis mice reduces lysosomal storage in CNS and extends lifespan. *Hum. Mol. Genet.* *24*, 4353–4364. <https://doi.org/10.1093/hmg/ddv168>.
- McCurdy, V.J., Johnson, A.K., Gray-Edwards, H.L., Randle, A.N., Brunson, B.L., Morrison, N.E., Salibi, N., Johnson, J.A., Hwang, M., Beyers, R.J., et al. (2014). Sustained normalization of neurological disease after intracranial gene therapy in a feline model. *Sci. Transl. Med.* *6*, 231ra48. <https://doi.org/10.1126/scitranslmed.3007733>.
- Baek, R.C., Broekman, M.L.D., Leroy, S.G., Tierney, L.A., Sandberg, M.A., d'Azzo, A., Seyfried, T.N., and Sena-Esteves, M. (2010). AAV-mediated gene delivery in adult GM1-gangliosidosis mice corrects lysosomal storage in CNS and improves survival. *PLoS One* *5*, e13468. <https://doi.org/10.1371/journal.pone.0013468>.
- Grieger, J.C., and Samulski, R.J. (2005). Packaging capacity of adeno-associated virus serotypes: impact of larger genomes on infectivity and postentry steps. *J. Virol.* *79*, 9933–9944. <https://doi.org/10.1128/jvi.79.15.9933-9944.2005>.
- Selot, R.S., Hareendran, S., and Jayandharan, G.R. (2014). Developing immunologically inert adeno-associated virus (AAV) vectors for gene therapy: possibilities and limitations. *Curr. Pharm. Biotechnol.* *14*, 1072–1082. <https://doi.org/10.2174/1389201015666140327141710>.
- Biffi, A., De Palma, M., Quattrini, A., Del Carro, U., Amadio, S., Visigalli, I., Sessa, M., Fasano, S., Brambilla, R., Marchesini, S., et al. (2004). Correction of metachromatic leukodystrophy in the mouse model by transplantation of genetically modified hematopoietic stem cells. *J. Clin. Invest.* *113*, 1118–1129. <https://doi.org/10.1172/jci200419205>.
- Visigalli, I., Delai, S., Politi, L.S., Di Domenico, C., Cerri, F., Mrak, E., D'Isa, R., Ungaro, D., Stok, M., Sanvito, F., et al. (2010). Gene therapy augments the efficacy of hematopoietic cell transplantation and fully corrects mucopolysaccharidosis type I phenotype in the mouse model. *Blood* *116*, 5130–5139. <https://doi.org/10.1182/blood-2010-04-278234>.
- Gleitz, H.F., Liao, A.Y., Cook, J.R., Rowston, S.F., Forte, G.M., D'Souza, Z., O'Leary, C., Holley, R.J., and Bigger, B.W. (2018). Brain-targeted stem cell gene therapy corrects mucopolysaccharidosis type II via multiple mechanisms. *Embo. Mol. Med.* *10*, e8730. <https://doi.org/10.15252/emmm.201708730>.
- Wakabayashi, T., Shimada, Y., Akiyama, K., Higuchi, T., Fukuda, T., Kobayashi, H., Eto, Y., Ida, H., and Ohashi, T. (2015). Hematopoietic stem cell gene therapy corrects neuropathic phenotype in murine model of mucopolysaccharidosis type II. *Hum. Gene Ther.* *26*, 357–366. <https://doi.org/10.1089/hum.2014.158>.
- Miwa, S., Watabe, A.M., Shimada, Y., Higuchi, T., Kobayashi, H., Fukuda, T., Kato, F., Ida, H., and Ohashi, T. (2020). Efficient engraftment of genetically modified cells is necessary to ameliorate central nervous system involvement of murine model of mucopolysaccharidosis type II by hematopoietic stem cell targeted gene therapy. *Mol. Genet. Metab.* *130*, 262–273. <https://doi.org/10.1016/j.ymgme.2020.06.007>.
- Wada, M., Shimada, Y., Iizuka, S., Ishii, N., Hiraki, H., Tachibana, T., Maeda, K., Saito, M., Arakawa, S., Ishimoto, T., et al. (2020). Ex-vivo gene therapy treats bone complications of mucopolysaccharidosis type II mouse models through bone remodeling reactivation. *Mol. Ther. Methods Clin. Dev.* *19*, 261–274. <https://doi.org/10.1016/j.omtm.2020.09.012>.
- Langford-Smith, A., Wilkinson, F.L., Langford-Smith, K.J., Holley, R.J., Sergijenko, A., Howe, S.J., Bennett, W.R., Jones, S.A., Wraith, J., Merry, C.L., et al. (2012). Hematopoietic stem cell and gene therapy corrects primary neuropathology and behavior in mucopolysaccharidosis IIIA mice. *Mol. Ther.* *20*, 1610–1621. <https://doi.org/10.1038/mt.2012.82>.

20. Sessa, M., Lorioli, L., Fumagalli, F., Acquati, S., Redaelli, D., Baldoli, C., Canale, S., Lopez, I.D., Morena, F., Calabria, A., et al. (2016). Lentiviral haemopoietic stem-cell gene therapy in early-onset metachromatic leukodystrophy: an ad-hoc analysis of a non-randomised, open-label, phase 1/2 trial. *Lancet* 388, 476–487. [https://doi.org/10.1016/s0140-6736\(16\)30374-9](https://doi.org/10.1016/s0140-6736(16)30374-9).
21. Gray-Edwards, H.L., Maguire, A.S., Salibi, N., Ellis, L.E., Voss, T.L., Diffie, E.B., Koehler, J., Randle, A.N., Taylor, A.R., Brunson, B.L., Denney, T.S., Beyers, R.J., Gentry, A.S., Gross, A.L., Batista, A.R., Sena-Esteves, M., and Martin, D.R. (2020). 7T MRI predicts amelioration of neurodegeneration in the brain after AAV gene therapy. *Mol. Ther. Methods Clin. Dev.* 17, 258–270. <https://doi.org/10.1016/j.omtm.2019.11.023>.
22. Malatack, J.J., Consolini, D.M., and Bayever, E. (2003). The status of hematopoietic stem cell transplantation in lysosomal storage disease. *Pediatr. Neurol.* 29, 391–403. [https://doi.org/10.1016/s0887-8994\(03\)00434-x](https://doi.org/10.1016/s0887-8994(03)00434-x).
23. Vogler, C., Levy, B., Grubb, J.H., Galvin, N., Tan, Y., Kakkis, E., Pavloff, N., and Sly, W.S. (2005). Overcoming the blood-brain barrier with high-dose enzyme replacement therapy in murine mucopolysaccharidosis VII. *Proc. Natl. Acad. Sci. U S A* 102, 14777–14782. <https://doi.org/10.1073/pnas.0506892102>.
24. Cho, S.Y., Lee, J., Ko, A.-R., Kwak, M.J., Kim, S., Sohn, Y.B., Park, S.W., and Jin, D.-K. (2015). Effect of systemic high dose enzyme replacement therapy on the improvement of CNS defects in a mouse model of mucopolysaccharidosis type II. *Orphanet. J. Rare Dis.* 10, 141. <https://doi.org/10.1186/s13023-015-0356-0>.
25. Conzelmann, E., and E., and Sandhoff, K. (1983). Partial enzyme deficiencies: residual activities and the development of neurological disorders. *Dev. Neurosci.* 6, 58–71. <https://doi.org/10.1159/000112332>.
26. Suzuki, Y., Ogawa, S., and Sakakibara, Y. (2009). Chaperone therapy for neuronopathic lysosomal diseases: competitive inhibitors as chemical chaperones for enhancement of mutant enzyme activities. *Perspect. Med. Chem.* 3, 7–19.
27. Matsuda, J., Suzuki, O., Oshima, A., Ogura, A., Noguchi, Y., Yamamoto, Y., Asano, T., Takimoto, K., Sukegawa, K., Suzuki, Y., and Naiki, M. (1997). Beta-galactosidase-deficient mouse as an animal model for GM1-gangliosidosis. *Glycoconjugate J.* 14, 729–736. <https://doi.org/10.1023/a:1018573518127>.
28. Itoh, M., Matsuda, J., Suzuki, O., Ogura, A., Oshima, A., Tai, T., Suzuki, Y., and Takashima, S. (2001). Development of lysosomal storage in mice with targeted disruption of the β -galactosidase gene: a model of human GM1-gangliosidosis. *Brain Dev.* 23, 379–384. [https://doi.org/10.1016/s0387-7604\(01\)00244-3](https://doi.org/10.1016/s0387-7604(01)00244-3).
29. Biffi, A., Capotondo, A., Fasano, S., Carro, U., Marchesini, S., Azuma, H., Malaguti, M.C., Amadio, S., Brambilla, R., Grompe, M., et al. (2006). Gene therapy of metachromatic leukodystrophy reverses neurological damage and deficits in mice. *J. Clin. Invest.* 116, 3070–3082. <https://doi.org/10.1172/jci28873>.
30. Petrillo, C., Calabria, A., Piras, F., Capotondo, A., Spinuzzi, G., Cuccovillo, I., Benedicenti, F., Naldini, L., Montini, E., Biffi, A., et al. (2019). Assessing the impact of cyclosporin A on lentiviral transduction and preservation of human hematopoietic stem cells in clinically relevant ex-vivo gene therapy settings. *Hum. Gene Ther.* 30, 1133–1146. <https://doi.org/10.1089/hum.2019.016>.
31. Heffner, G.C., Bonner, M., Christiansen, L., Pierciey, F.J., Campbell, D., Smurnyy, Y., Zhang, W., Hamel, A., Shaw, S., Lewis, G., et al. (2018). Prostaglandin E2 increases lentiviral vector transduction efficiency of adult human hematopoietic stem and progenitor cells. *Mol. Ther.* 26, 320–328. <https://doi.org/10.1016/j.ymthe.2017.09.025>.
32. Uchida, N., Nassehi, T., Drysdale, C.M., Gamer, J., Yapundich, M., Demirci, S., Haro-Mora, J.J., Leonard, A., Hsieh, M.M., and Tisdale, J.F. (2019). High-efficiency lentiviral transduction of human CD34+ cells in high-density culture with poloxamer and prostaglandin E2. *Mol. Ther. Methods Clin. Dev.* 13, 187–196. <https://doi.org/10.1016/j.omtm.2019.01.005>.
33. Sonoda, H., Morimoto, H., Yoden, E., Koshimura, Y., Kinoshita, M., Golovina, G., Takagi, H., Yamamoto, R., Minami, K., Mizoguchi, A., et al. (2018). A blood-brain-barrier-penetrating anti-human transferrin receptor antibody fusion protein for neuronopathic mucopolysaccharidosis II. *Mol. Ther.* 26, 1366–1374. <https://doi.org/10.1016/j.ymthe.2018.02.032>.
34. Narita, A., Shirai, K., Itamura, S., Matsuda, A., Ishihara, A., Matsushita, K., Fukuda, C., Kubota, N., Takayama, R., Shigematsu, H., et al. (2016). Ambroxol chaperone therapy for neuronopathic Gaucher disease: a pilot study. *Ann. Clin. Transl. Neur.* 3, 200–215. <https://doi.org/10.1002/acn3.292>.
35. Germain, D.P., Hughes, D.A., Nicholls, K., Bichet, D.G., Giugliani, R., Wilcox, W.R., Feliciani, C., Shankar, S.P., Ezgu, F., Amartino, H., et al. (2016). Treatment of fabry's disease with the pharmacologic chaperone migalastat. *N. Engl. J. Med.* 375, 545–555. <https://doi.org/10.1056/NEJMoa1510198>.
36. Matsuda, J., Suzuki, O., Oshima, A., Yamamoto, Y., Noguchi, A., Takimoto, K., Itoh, M., Matsuzaki, Y., Yasuda, Y., Ogawa, S., et al. (2003). Chemical chaperone therapy for brain pathology in GM1-gangliosidosis. *Proc. Natl. Acad. Sci. U S A* 100, 15912–15917. <https://doi.org/10.1073/pnas.2536657100>.
37. Hacein-Bey-Abina, S., Von Kalle, C., Schmidt, M., McCormack, M.P., Wulffraat, N., Leboulch, P., Lim, A., Osborne, C.S., Pawliuk, R., Morillon, E., et al. (2003). LMO2-Associated clonal T cell proliferation in two patients after gene therapy for SCID-X1. *Science* 302, 415–419. <https://doi.org/10.1126/science.1088547>.
38. Stein, S., Ott, M.G., Schultze-Strasser, S., Jauch, A., Burwinkel, B., Kinner, A., Schmidt, M., Krämer, A., Schwäble, J., Glimm, H., et al. (2010). Genomic instability and myelodysplasia with monosomy 7 consequent to EVI1 activation after gene therapy for chronic granulomatous disease. *Nat. Med.* 16, 198–204. <https://doi.org/10.1038/nm.2088>.
39. Cavazzana-Calvo, M., Payen, E., Negre, O., Wang, G., Hehir, K., Fusil, F., Down, J., Denaro, M., Brady, T., Westerman, K., et al. (2010). Transfusion independence and HMGA2 activation after gene therapy of human β -thalassaemia. *Nature* 467, 318–322. <https://doi.org/10.1038/nature09328>.
40. Jofra Hernández, R., Calabria, A., Sanvito, F., De Mattia, F., Farinelli, G., Scala, S., Visigalli, I., Carriglio, N., De Simone, M., Vezzoli, M., et al. (2021). Hematopoietic tumors in a mouse model of X-linked chronic granulomatous disease after lentiviral vector-mediated gene therapy. *Mol. Ther.* 29, 86–102. <https://doi.org/10.1016/j.ymthe.2020.09.030>.
41. Yanagisawa, M., Ariga, T., and Yu, R.K. (2006). Cholera toxin B subunit binding does not correlate with GM1 expression: a study using mouse embryonic neural precursor cells. *Glycobiology* 16, 19–22. <https://doi.org/10.1093/glycob/cwl003>.
42. Hahn, C.N., del Pilar Martin, M., del P., Schröder, M., Vanier, M.T., Suzuki, K., Hara, Y., Suzuki, K., and d'Azzo, A. (1997). Generalized CNS disease and massive GM1-ganglioside accumulation in mice defective in lysosomal acid β -galactosidase. *Hum. Mol. Genet.* 6, 205–211. <https://doi.org/10.1093/hmg/6.2.205>.
43. Kobayashi, H., Carbonaro, D., Pepper, K., Petersen, D., Ge, S., Jackson, H., Shimada, H., Moats, R., and Kohn, D.B. (2005). Neonatal gene therapy of MPS I mice by intravenous injection of a lentiviral vector. *Mol. Ther.* 11, 776–789. <https://doi.org/10.1016/j.ymthe.2004.10.006>.
44. Mitsuhashi, N., Fischer-Lougheed, J., Shulkin, I., Kleihauer, A., Kohn, D.B., Weinberg, K.I., Starnes, V.A., and Kearns-Jonker, M. (2006). Tolerance induction by lentiviral gene therapy with a nonmyeloablative regimen. *Blood* 107, 2286–2293. <https://doi.org/10.1182/blood-2005-03-1172>.
45. Kimura, T., Koya, R.C., Anselmi, L., Sternini, C., Wang, H.-J., Comin-Anduix, B., Prins, R.M., Faure-Kumar, E., Rozenzurg, N., Cui, Y., et al. (2007). Lentiviral vectors with CMV or MHCII promoters administered in vivo: immune reactivity versus persistence of expression. *Mol. Ther.* 15, 1390–1399. <https://doi.org/10.1038/sj.mt.6300180>.
46. Akiyama, K., Shimada, Y., Higuchi, T., Ohtsu, M., Nakauchi, H., Kobayashi, H., Fukuda, T., Ida, H., Eto, Y., Crawford, B.E., et al. (2014). Enzyme augmentation therapy enhances the therapeutic efficacy of bone marrow transplantation in mucopolysaccharidosis type II mice. *Mol. Genet. Metab.* 111, 139–146. <https://doi.org/10.1016/j.jymgme.2013.09.013>.
47. Hauser, E.C., Kasperzyk, J.L., d'Azzo, A., and Seyfried, T.N. (2004). Inheritance of lysosomal acid β -galactosidase activity and gangliosides in crosses of DBA/2J and knockout mice. *Biochem. Genet.* 42, 241–257. <https://doi.org/10.1023/b:bigi.0000034429.55418.71>.
48. Folch, J., Lees, M., and Stanley, G.S. (1957). A simple method for the isolation and purification of total lipids from animal tissues. *J. Biol. Chem.* 226, 497–509. [https://doi.org/10.1016/s0021-9258\(18\)64849-5](https://doi.org/10.1016/s0021-9258(18)64849-5).
49. Shimada, Y., Nishimura, E., Hoshina, H., Kobayashi, H., Higuchi, T., Eto, Y., Ida, H., and Ohashi, T. (2014). Proteasome inhibitor bortezomib enhances the activity of multiple mutant forms of lysosomal α -glucosidase in pompe disease. *JIMD Rep.* 18, 33–39. https://doi.org/10.1007/8904_2014_345.